Viscosity, Interfacial Tension, Density, and Refractive Index of Ionic Liquids [EMIM][$MeSO_3$], [EMIM][$MeOHPO_2$], [EMIM][$OcSO_4$], and [BBIM][NTf_2] in Dependence on Temperature at Atmospheric Pressure†

Benjamin Hasse,‡ Julia Lehmann,‡ Daniel Assenbaum,|| Peter Wasserscheid,|| Alfred Leipertz,§ and Andreas Paul Fröba*,‡

Erlangen Graduate School in Advanced Optical Technologies, University of Erlangen-Nuremberg, Paul-Gordan-Straβe 6, D-91052 Erlangen, Germany, Institute of Chemical and Bioengineering, Department of Engineering Thermodynamics, University of Erlangen-Nuremberg, Am Weichselgarten 8, D-91058 Erlangen, Germany, and Institute of Chemical and Bioengineering, Department of Chemical Reaction Engineering, University of Erlangen-Nuremberg, Egerlandstraβe 3, D-91058 Erlangen, Germany

This work represents a continuation of former investigations, where viscosity, interfacial tension, density, and refractive index of ionic liquids (ILs) [EMIM][$EtSO_4$] (1-ethyl-3-methylimidazolium ethylsulfate), [EMIM][NTf_2] (1-ethyl-3-methylimidazolium bis(trifluoromethylsulfonyl)imide), [EMIM][$N(CN)_2$] (1-ethyl-3-methylimidazolium dicyanamide), and [OMA][NTf_2] (trioctylmethylammonium bis(trifluoromethylsulfonyl)imide) were studied. Here, the ILs [EMIM][$MeSO_3$] (1-ethyl-3-methylimidazolium methanesulfonate), [EMIM][$MeOHPO_2$] (1-ethyl-3-methylimidazolium methylphosphonate), [EMIM][$OcSO_4$] (1-ethyl-3-methylimidazolium octylsulfate), and [BBIM][NTf_2] (1-butyl-3-butylimidazolium bis(trifluoromethylsulfonyl)imide) were investigated again both by conventional techniques and by surface light scattering (SLS). An Abbe refractometer was used for the measurement of the refractive index in the range of (283.15 to 313.15) K with an expanded uncertainty ($k = 2$) of about 0.0005. The density was measured between (273.15 and 313.15) K with a vibrating tube densimeter and an expanded uncertainty ($k = 2$) of about 0.02 %. The interfacial tension was obtained from the pendant drop technique at a temperature of 293.15 K with an expanded uncertainty ($k = 2$) of 1 %. On the basis of this datum and the temperature dependence of density, the interfacial tension for all relevant temperatures was estimated via an appropriate prediction model. For the ILs studied within this work, at a first-order approximation, the quantity directly accessible by SLS was the ratio of dynamic viscosity to surface tension. Combining the results from SLS with values for density and interfacial tension from conventional methods, the dynamic viscosity could be obtained from (273.15 to 333.15) K with an estimated expanded uncertainty ($k = 2$) of less than 3 %. Besides a comparison with the literature, the major aim of this work was to point out the influence of variations of the anion on thermophysical properties of $[EMIM]^+$-based ILs. In addition, the effect of different cations was studied in ILs with the $[NTf_2]^-$ anion. ILs with equal cations and similar anions can still exhibit different properties, which is interpreted with relevant molecular interactions.

Introduction

At present, due to an increasing importance of ionic liquids (ILs) in many fields of technology, a large number of publications dealing with the thermophysical properties of these low-temperature molten salts can be found in the literature. Due to an almost unlimited number of potential combinations of cations and anions, ILs can be tailored to specific applications.[1−7] Most of the studies on the thermophysical properties of ILs in the literature dedicated to characterize these after their synthesis. Thus, for many thermophysical properties of ILs, only a single datum near room temperature, usually (293 or 298) K, and atmospheric pressure is reported. Although there seems to be neither need nor time to achieve the highest accuracy in the measurement of the thermophysical properties of ILs, the accuracy achieved must be known. This aspect is often ignored in existing research activities for ILs. It is fairly common to find differences between published data sets, which are more than 1 order of magnitude larger than the combined uncertainties of the measurements. This situation holds both for equilibrium data and for transport properties, whereas it is more pronounced for the latter. The disagreement between the different data sources may be attributed to inconsistent sample purity,[8−12] yet this seems not to be the only reason. The discrepancies between different sources are also found to be influenced by inconsistent experimental techniques, the use of routine laboratory-analytic methods, e.g., rotational and rolling-ball viscometers, as well as by an inadequate estimation of the uncertainty. The current situation is hindering both a more fundamental understanding of the structure−property relationships of ILs as well as their successful and large-scale application.

In a former work,[13] we have shown that surface light scattering (SLS) can provide reliable viscosity data for ILs. For [EMIM][$EtSO_4$] (1-ethyl-3-methylimidazolium ethylsulfate), [EMIM][NTf_2] (1-ethyl-3-methylimidazolium bis(trifluoro-

* Author to whom correspondence should be addressed. Tel.: +49-9131-85-29789. Fax: +49-9131-85-29901. E-mail: apf@aot.uni-erlangen.de.
† Part of the "William A. Wakeham Festschrift".
‡ Erlangen Graduate School in Advanced Optical Technologies.
§ Department of Engineering Thermodynamics.
|| Department of Chemical Reaction Engineering.

10.1021/je900134z CCC: $40.75
Published on Web 04/01/2009

Table 1. Molecular Weight M, Concentration of Water by Mass w, and Nominal Purity of Ionic Liquids [EMIM][$MeSO_3$], [EMIM][$MeOHPO_2$], [EMIM][$OcSO_4$], and [BBIM][NTf_2] Studied in This Work

	[EMIM][$MeSO_3$]	[EMIM][$MeOHPO_2$]	[EMIM][$OcSO_4$]	[BBIM][NTf_2]
M/g·mol^{-1}	206.26	206.18	320.45	461.44
w/ppm	1312 ± 262	284 ± 57	1116 ± 223	136 ± 27
purity/%	> 99	> 98	> 99	> 99

methylsulfonyl)imide), [EMIM][$N(CN)_2$] (1-ethyl-3-methylimidazolium dicyanimide), and [OMA][NTf_2] (trioctylmethylammonium bis(trifluoromethylsulfonyl)imide), we have determined the viscosity over a temperature range from (273 to 333) K at atmospheric pressure with an estimated expanded uncertainty (k = 2) of less than 3 %. This work represents a continuation of this previous study and provides again, besides interfacial tension, density, and refractive index, reliable data for the dynamic viscosity of a selected set of pure ILs. In comparison to conventional viscometers, the main advantage of the SLS technique relies on the possibility of determining the viscosity in macroscopic thermodynamic equilibrium, and this in an absolute way, without the need of any calibration procedure involving a fluid of known viscosity.[14−16] The objects of investigation were now four imidazolium-based ILs, [EMIM][$MeSO_3$] (1-ethyl-3-methylimidazolium methanesulfonate), [EMIM][$MeOHPO_2$] (1-ethyl-3-methylimidazolium methylphosphonate), [EMIM][$OcSO_4$] (1-ethyl-3-methylimidazolium octylsulfate), and [BBIM][NTf_2] (1-butyl-3-butylimidazolium bis(trifluoromethylsulfonyl)imide). Taking into account also the ILs investigated previously,[13] the influence of variations of the anion on thermophysical properties of [EMIM]-based ILs and the effect of changing the cation in ILs with [NTf_2]-anion should be pointed out.

The following experimental section gives some information about the used conventional techniques and an extended outline of the SLS theory. After a description of the sample preparation procedure, experimental conditions, and achieved uncertainties, the results for refractive index, density, interfacial tension, and dynamic viscosity are discussed subsequently concerning the influence of structural variations on the thermophysical properties. At the end of each subsequence, data obtained in the present work are compared with literature data.

Experimental Section

Materials and Sample Preparation Procedure. [EMIM][$EtSO_4$], [Li][NTf_2], [EMIM][$MeSO_3$], and butylimidazole were purchased from Solvent Innovation GmbH, Cologne, Germany, with a nominal purity higher than 99 %. [EMIM][$MeOHPO_2$] was purchased from Solvent Innovation GmbH, Cologne, Germany, with a nominal purity higher than 98 %. [EMIM][$OcSO_4$] was synthesized by reacting [EMIM][$EtSO_4$] with n-octanol with the procedure described by Himmler et al.[17] [BBIM][NTf_2] was synthesized by reacting equal amounts of [BBIM][Br] with [Li][NTf_2] in aqueous solution at room temperature under heavy stirring. The upper aqueous phase and the lower ionic liquid phase were separated by decantation. The upper phase was disposed, and the lower phase was washed with distilled water three times and dried under reduced pressure at 70 °C. The [BBIM][Br] was obtained by a reaction of butylimidazole with 1-bromobutane as described by Davis et al.[18] The purity of [EMIM][$OcSO_4$] and [BBIM][NTf_2] was proved by ^{1}H NMR analysis (JEOL, ECX +400 spectrometer) in dimethylsulfoxide-d_6 (DMSO-d_6) as solvent. The total peak integral in the ^{1}H NMR spectrum was found to correspond to a nominal purity higher than 99 %. Before use, the ILs were dried at about 333.15 K for a time period of at least 4 h on a vacuum line (0.5 mbar) with an oil-sealed vacuum pump and a liquid nitrogen trap. For the dried ILs, the concentration of water was proved twice by Karl Fischer coulometric titration (Metrohm, 756 KF Coulometer) just before filling of the sample cell and after the SLS experiments. The expanded uncertainty (k = 2) of the water content determinations performed within this work is estimated to be less than ± 20 %. The molecular weight, nominal purity, and water content of the ILs studied in this work are summarized in Table 1. Here, the water content was obtained from the average of the respective two water content measurements. For all ILs investigated, the change in the water content was within the experimental uncertainty of the used Karl Fischer coulometric titration method. All parts of the measuring devices, which were in contact with the sample, as well as all glassware used for sample handling were cleaned, rinsed with double-distilled water, and oven-dried.

Abbe Refractometer: Refractive Index. The refractive index n_D at the sodium line (λ_D = 589.3 nm) and the refractive index difference $n_F - n_C$ for the Fraunhofer lines F (λ_F = 486.1 nm) and C (λ_C = 656.3 nm) were measured with an Abbe refractometer (Leo Kuebler, R 6000 G). The temperature of the samples was controlled with a laboratory thermostat within ± 0.1 K and measured by a mercury thermometer with an uncertainty of ± 0.5 K. The refractometer was calibrated with water, and its expanded uncertainty (k = 2) in the measurement of the refractive index is estimated to be less than ± 0.0005.

Vibrating Tube Method: Density. Density measurements at atmospheric pressure are based on the vibrating tube method. For the density meter (Anton Paar, DMA 5000) used here, long-term drift is eliminated by a reference oscillator built into the measuring cell, and only one adjustment at 293.15 K is sufficient to reach a high accuracy for the whole measuring temperature range. The DMA 5000 allows a full-range viscosity correction, whereby all viscosity related errors inherent to all known types of oscillating U-tube density meters are automatically eliminated. The temperature of the U-tube is controlled within ± 1 mK and measured by a high-precision platinum resistance probe with an uncertainty of ± 10 mK. For the density meter calibration, standard water and air were used. The expanded uncertainty (k = 2) of the present density measurements for ILs is estimated to be less than ± 0.02 %. For this, the calibration error of the apparatus of 0.01 % and the error associated with the following measurement procedure for ILs have been taken into account. The precision or repeatability of the instrument was better than ± 0.001 %.

Pendant Drop Technique: Interfacial Tension. For the evaluation of the dynamic viscosity from SLS, interfacial tension data are needed in the case of fluids of high viscosity and/or low interfacial tension. For an accurate determination of the dynamic viscosity of high viscosity fluids, however, one has to ensure that the liquid surface under investigation corresponds to the interfacial tension values used for data evaluation. This was ensured by investigating identical samples of ILs by SLS and the pendant drop method for measuring the interfacial tension. Here, a universal surface

analyzer (OEG, SURFTENS universal) was used, where the geometrical profile of a pendant drop is compared with the theoretical drop profile obtained from the Laplace equation. The measurements were performed inside an optical glass cell for photometry (Hellma, 402.000) at well-defined conditions for a temperature of (293.15 ± 0.1) K. For the interfacial tension data of all ILs, the expanded uncertainty ($k = 2$) was estimated to be less than ± 1 %.

Surface Light Scattering (SLS): Viscosity. Here, a more specific treatment of the theory of SLS was used, by inspecting the hydrodynamic capillary wave problem in the limiting case of a free liquid surface, neglecting the presence of a second fluid phase. For the present investigations of a phase boundary between an IL and air at atmospheric pressure, this can be done without any significant loss of accuracy because the vapor properties are very small compared to the respective liquid quantities.[16] In this case, the decay dependence on time t of a particular surface mode of the form $\exp[\mathrm{i}\,\vec{q}\,\vec{r} + \mathrm{i}\alpha\, t]$, with a wave vector $\vec{q}$ at a given point $\vec{r}$, is obtained from the dispersion equation[19]

$$\left(\mathrm{i}\alpha + \frac{2\eta q^2}{\rho}\right)^2 + \frac{\sigma q^3}{\rho} + gq - \frac{4\eta^2 q^4}{\rho^2}\sqrt{1 + \frac{\mathrm{i}\alpha\rho}{\eta q^2}} = 0 \quad (1)$$

where g is the acceleration of gravity and η, σ, and ρ are the dynamic viscosity, interfacial tension, and density of the liquid, respectively. In general, two physical solutions for the temporal decay of surface fluctuations and thus for the complex frequency α have to be considered. In the case of low viscosity and/or large interfacial tension, surface fluctuations show an oscillatory behavior corresponding to the complex frequency $\alpha_{1,2} = \pm\,\omega_q + \mathrm{i}\Gamma$, where the real part represents the frequency ω_q and the imaginary part the damping Γ of the surface mode observed. In the case of high viscosity and/or low interfacial tension, as was relevant within this work, surface fluctuations are overdamped and do not propagate ($\omega_q = 0$). In this case, the complex frequency is associated with two different damping rates, $\alpha_{1,2} = \mathrm{i}\Gamma_{1,2}$. As a first-order approximation, the complex frequency can be represented by

$$\alpha_{1,2} \approx \pm\sqrt{\frac{\sigma q^3}{\rho} + gq} + \mathrm{i}\frac{2\eta q^2}{\rho} \quad (2)$$

or

$$\alpha_1 \approx \mathrm{i}\frac{q}{2\eta}\left(\sigma + \frac{g\rho}{q^2}\right) \text{ and } \alpha_2 \approx \mathrm{i}0.9\frac{\eta q^2}{\rho} \quad (3)$$

assuming that the decay of surface waves is oscillatory or overdamped, respectively. In principle, for both cases viscosity and interfacial tension can be determined simultaneously by probing frequency and/or damping of surface fluctuations within the SLS experiment. In the case of an oscillatory behavior this is a straightforward task, and the SLS technique is well-established for measuring viscosity and surface tension with high accuracy.[14] In the overdamped case, only under special conditions can both properties be accessed simultaneously.[20] For the ILs investigated in this experiment, over the temperature range (273.15 to 333.15) K, however, from the two modes decaying at different rates, only the one associated with α_1 could be resolved. Thus, as a first-order approximation and neglecting the forces of inertia, cf., eq 3, SLS gives only access to the ratio of dynamic viscosity η to interfacial tension σ. For this purpose, the decay behavior or mean lifetime $\tau_{C,1}$, $\tau_{C,1} = 1/\Gamma_1 \approx 2\,\eta/(\sigma q)$, of surface fluctuations at a given wavenumber q is analyzed. For a detailed and comprehensive description of the fundamentals and methodological principles of SLS, the reader is referred to the specialized literature.[14,19,21−23]

The experimental setup used here for the investigation of the ILs is the same as that employed in our former SLS investigations for different ILs[13] and includes a laser (Coherent, Verdi-V2; laser wavelength in vacuo $\lambda_0 = 532$ nm; operated at 500 mW), correlator (ALV, Fast-Corr 6/256), optical and electro-optical parts, sample cell (aluminum; inner diameter, 70 mm; volume, 150 cm^3), and thermostat. Scattered light is detected in the forward direction near refraction perpendicular to the surface plane at variable and relatively high wave numbers. For this arrangement, the modulus of the wave vector, $q = 2\,\pi\,/\lambda_0 \sin(\Theta_E)$, of the observed surface vibration mode can be deduced as a function of the easily accessible angle of incidence Θ_E. For the experiment, the angle of incidence Θ_E was set between (3.0 and 4.2)° and measured with a high precision rotation table with an uncertainty of ± 0.005°. The temperature of the cell was measured with two calibrated 100 Ω platinum resistance probes integrated into the main body of the vessel, with a resolution of 0.25 mK, using an ac bridge (Anton Paar, MKT 100). The uncertainty of the absolute temperature measurement was less than ± 15 mK. The temperature stability during an experimental run was better than ± 1 mK. For each temperature, at least six measurements at different angles of incidence were performed.

In the present work, however, data for the dynamic viscosity η of the ILs were obtained by an exact numerical solution of the dispersion relation eq 1. For this, data obtained for the dynamics of surface waves, i.e., the mean lifetime $\tau_{C,1}$ at a defined wave vector q, were combined with reference data for the interfacial tension σ and density ρ. For the latter, even approximate or less accurate values with an uncertainty of ± 10 % allow a successful determination of the dynamic viscosity. Although the use of eq 3 for data evaluation does not allow the determination of the dynamic viscosity with high accuracy, the approximation can be applied to get a good estimate for the uncertainty of our SLS results in an analytical manner by combining in quadrature the errors for the interfacial tension σ, mean lifetime $\tau_{C,1}$, and wave vector q. Taking into account relative uncertainties of clearly less than (± 0.5, ± 0.15, and ± 1) % for the mean lifetime $\tau_{C,1}$, wave vector q, and interfacial tension σ, respectively, the expanded uncertainty ($k = 2$) of our values for the dynamic viscosity η is estimated to be less than ± 3.0 %.

Results and Discussion

In the following, the results for refractive index, density, interfacial tension, and dynamic viscosity are discussed in subsequences. First, the obtained data will be interpreted in connection with the intermolecular interactions present in ILs. Thereafter, the respective thermophysical properties are compared to available literature. In general, for the ILs investigated in this work, a lack of literature data can be found.

Refractive Index. The measured data for the refractive index n_D and the refractive index difference $n_F - n_C$ for the ILs [EMIM][$MeSO_3$], [EMIM][$MeOHPO_2$], [EMIM][$OcSO_4$], and [BBIM][NTf_2] in the temperature range from (283.15 to 313.15) K at atmospheric pressure are summarized in Table 2 and shown

Table 2. Refractive Index n_D and Refractive Index Difference $n_F - n_C$ of [EMIM][MeSO$_3$], [EMIM][MeOHPO$_2$], [EMIM][OcSO$_4$], and [BBIM][NTf$_2$] from T = (283.15 to 313.15) K at Atmospheric Pressure

	[EMIM][MeSO$_3$]		[EMIM][MeOHPO$_2$]		[EMIM][OcSO$_4$]		[BBIM][NTf$_2$]	
T/K	n_D	$n_F - n_C$	n_D	$n_F - n_C$	n_D	$n_F - n_C$	n_D	$n_F - n_C$
283.15	1.5018	0.0104	1.4969	0.0110	1.4786	0.0089	1.4376	0.0075
293.15	1.4996	0.0100	1.4935	0.0109	1.4766	0.0095	1.4347	0.0076
303.15	1.4977	0.0101	1.4928	0.0106	1.4737	0.0095	1.4324	0.0078
313.15	1.4949	0.0101	1.4902	0.0102	1.4712	0.0093	1.4298	0.0081

in Figure 1. The refractive index n can be calculated by the linear equation

$$n = n_0 + n_1 T + \frac{\Delta n}{\Delta \lambda}(\lambda - \lambda_D) \quad (4)$$

where T represents the temperature in K, λ the wavelength in m, and λ_D (= 589.3·10^{-9} m) the wavelength of the sodium vapor line. The fit parameters of eq 4, n_0 and n_1, as well as the mean dispersion $\Delta n/\Delta\lambda$ are given in Table 3. The latter corresponds to the average value of the refractive index differences $n_F - n_C$ and is assumed to be independent of temperature. For all ILs, the deviations of the experimental refractive index data n_D from their correlation according to eq 4 are clearly within the measurement uncertainty of ± 0.0005.

Deetlefs et al.[24] and Brocos et al.[25] report that the larger the reduced molar free volume, i.e., the unoccupied part of the molar volume of a substance, the smaller its refractive index is, which is in good agreement with the behavior of the refractive indices of the investigated ILs. For all [EMIM]-based ILs in this and the previous work,[13] an increasing refractive index with decreasing molar free volume is found. Furthermore, when taking the refractive indices of the ILs containing the [NTf$_2$]-anion into consideration, again an increasing refractive index with decreasing molar free volume is assessed.

For comparison, only two data points are available in the literature for the refractive index of the ILs investigated in this work. Arce et al.[26] report for [EMIM][MeSO$_3$] at 298.15 K a refractive index of 1.49549, which differs about −0.2 % from the refractive index obtained in our experiments. Their value was obtained with an Abbe refractometer (ATAGO, RX-5000) with an uncertainty of ± 0.00001. Deenadayalu et al.[27] report for [EMIM][OcSO$_4$] at 298.2 K and atmospheric pressure a value of 1.4710, which is about 0.27 % lower than the datum of this work. The authors give no information about the used measuring technique and its uncertainty. The literature data are clearly outside the expanded uncertainty (k = 2) of about ± 0.0005 of this work. Besides different sample purities, this may be caused also by an overestimation of experimental accuracy.

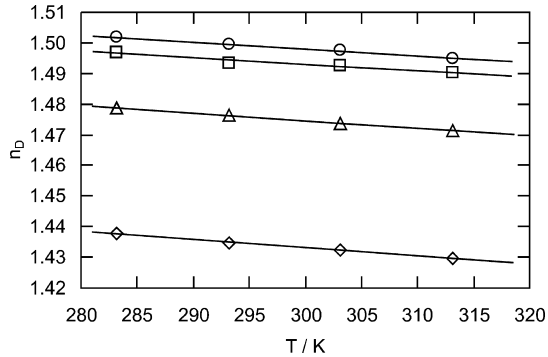

Figure 1. Refractive index n_D of ionic liquids at atmospheric pressure as a function of temperature: ○, [EMIM][MeSO$_3$]; □, [EMIM][MeOHPO$_2$]; △, [EMIM][OcSO$_4$]; ◇, [BBIM][NTf$_2$].

Table 3. Fit Parameters n_0, n_1, and $\Delta n/\Delta\lambda$ of Equation 4 for the Calculation of the Refractive Index n for Ionic Liquids [EMIM][MeSO$_3$], [EMIM][MeOHPO$_2$], [EMIM][OcSO$_4$], and [BBIM][NTf$_2$]

	n_0	n_1/K^{-1}	$\Delta n/\Delta\lambda$/m^{-1}	rms[a]
[EMIM][MeSO$_3$]	1.56597	−0.000226	−59618	0.013
[EMIM][MeOHPO$_2$]	1.55512	−0.000207	−62774	0.037
[EMIM][OcSO$_4$]	1.54947	−0.000250	−54626	0.012
[BBIM][NTf$_2$]	1.51048	−0.000258	−45484	0.008

[a] Standard percentage deviation of n_D to the fit.

Density. Our experimental density data obtained for temperatures between (273.15 and 363.15) K at atmospheric pressure are summarized in Table 4 and in Figure 2. The densities for all investigated ILs can be represented by a polynomial of second order

$$\rho = \rho_0 + \rho_1 T + \rho_2 T^2 \quad (5)$$

where all data have been taken into account with the same statistical weight. In eq 5, T is the temperature in K and ρ_0, ρ_1, and ρ_2 are the fit parameters given in Table 5. For all ILs, the deviations of the experimental density data from their correlation according to eq 5 lie clearly within the measurement uncertainty of ± 0.02 %.

Fredlake and co-workers[28] describe decreasing densities with increasing size of the cation. For the influence of the anion on the density, they report that an increasing molar weight of the anion causes an increase of density for anions that are small enough to easily occupy close-approach positions around the relatively large cation. For the [EMIM]-based ILs investigated in this and the previous work,[13] the density increases with increasing molecular weight of the respective anions. Only for the two ILs [EMIM][MeSO$_3$] and [EMIM][OcSO$_4$] the densities do not match this behavior. For [EMIM][OcSO$_4$], this can be explained with the long C$_8$ side chain of the anion, which prohibits the formation of tight molecular assemblies leading to a lower density. Yet, for [EMIM][MeSO$_3$], the observed high density cannot be explained in that way. The high density may be attributed to the quite symmetrical molecular structure, which can lead to the formation of a gridlike assembly of anions and cations, where present hydrogen bonding shortens intermolecular distances. Comparing the ILs containing the [NTf$_2$]-anion, the results are in good agreement with the observations of Fredlake and co-workers.[28] The IL with the largest [OMA]-cation exhibits the lowest density, followed by the IL containing the [BBIM]-cation. The smallest [EMIM]-cation leads to the highest density. Tokuda et al.[29] also found a decreasing density with increasing alkyl chain length in ILs containing 1-alkyl-3-methylimidazolium cations.

For [EMIM][MeSO$_3$], Cooper and O'Sullivan[30] report for a temperature of 298 K a density of 1.240 g·cm^{-3}, which was obtained from volumetric measurements. They give no further

Table 4. Density ρ of Ionic Liquids [EMIM][$MeSO_3$], [EMIM][$MeOHPO_2$], [EMIM][$OcSO_4$], and [BBIM][NTf_2] from T = (273.15 to 363.15) K at Atmospheric Pressure

	[EMIM][$MeSO_3$]	[EMIM][$MeOHPO_2$]	[EMIM][$OcSO_4$]	[BBIM][NTf_2]
T/K	ρ/kg·m^{-3}	ρ/kg·m^{-3}	ρ/kg·m^{-3}	ρ/kg·m^{-3}
273.15	1259.14	1208.75	1111.56	1362.73
278.15	1255.59	1205.29	1108.00	1358.06
283.15	1252.04	1201.82	1104.34	1353.51
288.15	1248.49	1198.42	1100.82	1349.01
293.15	1244.96	1195.12	1097.48	1344.50
298.15	1241.52	1191.82	1094.15	1340.01
303.15	1238.15	1188.50	1090.83	1335.51
308.15	1234.77	1185.21	1087.52	1331.02
313.15	1231.40	1181.92	1084.20	1326.56
318.15	1228.03	1178.65	1080.97	1322.09
323.15	–	1175.39	–	–
328.15	1221.33	1172.14	1074.55	1313.20
333.15	1218.00	1168.89	1071.34	1308.77
338.15	1214.69	1165.66	1068.14	1304.36
343.15	1211.38	1162.45	1064.94	1299.99
348.15	1208.09	1159.25	1061.76	1295.57
353.15	1204.82	1156.06	1058.59	1291.20
358.15	1201.56	1152.90	1055.42	1286.84
363.15	1198.31	1149.73	1052.26	1282.50

information about the measurement technique and the uncertainty. Himmler et al.[31] report also a value of 1.24 g·cm^{-3}, obtained with a pycnometer at an unspecified "room temperature". Arce et al.[26] obtained a value of 1.24373 g·cm^{-3} at 298.15 K with a vibrating tube densimeter (Anton Paar, DMA 60-602) with an uncertainty of ± 0.00004 g·cm^{-3}. Taking into account both the error connected with the calibration and that of the subsequent measuring procedure, this uncertainty seems to be underestimated, i.e., below the expected value. The differences between the literature data and the data obtained in this work for [EMIM][$MeSO_3$] are always larger than the combined expanded estimated uncertainty of the measurements. This statement also holds for the comparison of the literature data among themselves. For the density of [EMIM][$OcSO_4$], only Himmler et al.[17] provide a single value of 1.10 g·cm^{-3} measured with a pycnometer at "room temperature". Their datum deviates about 0.5 % from the data correlation of this work. At present, neither for [EMIM][$MeOHPO_2$] nor for [BBIM][NTf_2] are density data available in the literature.

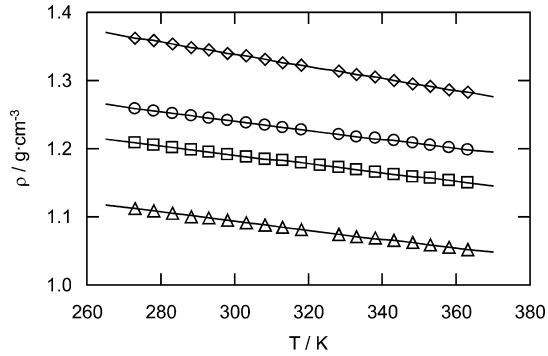

Figure 2. Liquid density ρ of ionic liquids at atmospheric pressure as a function of temperature: ○, [EMIM][$MeSO_3$]; □, [EMIM][$MeOHPO_2$]; △, [EMIM][$OcSO_4$]; ◇, [BBIM][NTf_2].

Table 5. Coefficients of Equation 5 for the Density of Ionic Liquids [EMIM][$MeSO_3$], [EMIM][$MeOHPO_2$], [EMIM][$OcSO_4$], and [BBIM][NTf_2] Listed in Table 4

	ρ_0/kg·m^{-3}	ρ_1/kg·m^{-3}·K^{-1}	ρ_2/kg·m^{-3}·K^{-2}	rms[a]
[EMIM][$MeSO_3$]	1478.846	−0.90298	0.35975·10^{-3}	0.0044
[EMIM][$MeOHPO_2$]	1415.782	−0.83656	0.28644·10^{-3}	0.0033
[EMIM][$OcSO_4$]	1335.748	−0.94722	0.45986·10^{-3}	0.0098
[BBIM][NTf_2]	1630.002	−1.04499	0.24251·10^{-3}	0.0018

[a] Standard percentage deviation of ρ to the fit.

Interfacial Tension. Table 6 summarizes the values obtained for interfacial tension within this work at a single temperature of 293.15 K at atmospheric pressure. As mentioned in the Experimental Section, these values are needed together with the temperature dependence of the density to predict the interfacial tension in the range of (273.15 to 333.15) K, shown in Figure 3, and to evaluate the dynamic viscosity from the SLS experiments. The prediction method is based on the MacLeod−Sudgen correlation given in ref 32. MacLeod[33] suggested a relation between the interfacial tension σ, the liquid density ρ_l, and vapor density ρ_v, $\sigma^{1/4} = C(\rho_l - \rho_v)$, where C is a constant. Sugden[34] modified MacLeod's expression and introduced the temperature-independent parameter, the parachor, $P = CM$, which can be estimated from the structure of the molecule. Investigating ILs, the existence of a vapor phase inside the measurement cell can be neglected. Thus, for the prediction of the temperature dependency of interfacial tension, only a single experimental value for the interfacial tension at an arbitrary temperature and the knowledge of the temperature dependency of the density is needed. The interfacial tension σ at any temperature in this work was predicted by

$$\sigma = \sigma_{20°C}(\rho/\rho_{20°C})^4 \quad (6)$$

where $\sigma_{20°C}$ and $\rho_{20°C}$ are the measured interfacial tension and density at the reference temperature of 20 °C. The proposed prediction scheme represents the interfacial tension of high viscosity fluids typically with an uncertainty of less than 2 %, which was tested for several reference fluids; see, e.g., ref 15.

Until now, only a limited number of studies about the interfacial tension of ILs has been available in the literature. Law and Watson[35] found that with increasing alkyl chain length of the cation ILs show decreasing interfacial tension values. Furthermore, they revealed that the interfacial tension of ILs containing the same cation increases with increasing molecular size of the anion, which were highly symmetrical molecules in their study. The results found for the ILs containing the [NTf_2]-anion comply well with their first finding. [OMA][NTf_2] with the largest cation exhibits the lowest interfacial tension, followed by [BBIM][NTf_2], and last by [EMIM][NTf_2] with the highest

Table 6. Interfacial Tension $\sigma_{20°C}$ of Ionic Liquids [EMIM][$MeSO_3$], [EMIM][$MeOHPO_2$], [EMIM][$OcSO_4$], and [BBIM][NTf_2] at $T = 293.15$ K and Atmospheric Pressure

	[EMIM][$MeSO_3$]	[EMIM][$MeOHPO_2$]	[EMIM][$OcSO_4$]	[BBIM][NTf_2]
$\sigma_{20°C}$/mN·m^{-1}	50.72	45.49	31.00	29.55

interfacial tension and the smallest cation. For the [EMIM]-based ILs, our results do not agree with the second finding of Law and Watson.[35] [EMIM][$OcSO_4$] with the largest anion shows the lowest interfacial tension of all [EMIM]-based ILs. In contrast, the very small [$MeSO_3$]-anion leads to the highest interfacial tension. Therefore, the interfacial tension of ILs containing the same cation has to be strongly influenced by the strength of electrostatic interactions between the anion and cation. Referring to Tokuda et al.,[36] these interactions are governed by the Lewis basicity of the anion. They also found the Lewis basicity to be high for anions having locally large negative charges with an asymmetric distribution and to be low for anions having symmetrically distributed low negative charges. In this context, the highest interfacial tension found for [EMIM][$MeSO_3$] can be explained by the anion's strong negative charge and the lowest charge delocalization. [EMIM]-[$EtSO_4$] exhibits the second highest value, as the negative charge of [$EtSO_4$] is weaker compared to [$MeSO_3$]. [EMIM]-[$MeOHPO_2$] has a lower interfacial tension than [EMIM] [$EtSO_4$], although [$MeOHPO_2$] should have a higher basicity than [$EtSO_4$]. A possible explanation for this behavior might be the lower molecular size of [$MeOHPO_2$] in comparison to [$EtSO_4$] which is superior to the influence of the Lewis basicity. The second lowest interfacial tension found for [EMIM][NTf_2] can be explained by the symmetrical delocalization of the weak negative charge in the anion. For [EMIM][$OcSO_4$], the size of the alkyl chain of the anion prevents the formation of strong electrochemical interactions between the anion and cation, which leads to a very low interfacial tension.

For the interfacial tension, a comparison of our data with experimental data from the literature could not be drawn. Here, a comparison was performed with calculated values based on a quantitative structure−property relationship (QSPR) using parachor contribution data for neutral compounds by Knotts et al.[37] and Sewell.[38] Therefore, information about the molecular weight M and density ρ was required and adopted from Table 1 and eq 5. The interfacial tension data calculated from the parachor contribution data deviate with respect to eq 6 constantly, −12.2 %, −32.8 %, −44.2 %, and −16.5 % for [EMIM][$MeSO_3$], [EMIM][$MeOHPO_2$], [EMIM][$OcSO_4$], and [BBIM][NTf_2], respectively. The constant offset between our predicted values, eq 6, and the corresponding data by Knotts et al.[37] and Sewell[38] is attributable to the consistent density values, eq 5, used for both predictions. The large deviations may be found in the neutral parachor contribution data, which do not include ionic interactions, even though they are present in the systems investigated here.

Viscosity. The results for the dynamic viscosity from SLS at temperatures between (273.15 and 333.15) K at atmospheric pressure are shown in Figure 4 and Table 7. Each data point represents the average of at least six independent measurements with a different modulus of the wave vector q. The experimental data can well be represented in the form of a Vogel equation,

$$\eta = \eta_0 \exp[B/(T - C)] \tag{7}$$

where T is the temperature in K and η_0, B, and C are the fit parameters given in Table 8. Here, also the standard deviation (root-mean-square, rms) of our data relative to those calculated by eq 7 is listed. For the data correlation, the statistical weight of each data point has been assumed to be the same. The residuals of the viscosity data from the fit, eq 7, are clearly smaller than the expanded uncertainty ($k = 2$) of less than ± 3 %. It should be noted that for our viscosity data at 293.15 K, due to the lower uncertainty of the surface tension data used for data evaluation of the SLS experiment, even a lower expanded uncertainty ($k = 2$) of less than ± 2 % can be stated.

In general, the viscosity of ILs is governed besides the entanglement between the molecules by Coulomb forces like van der Waals interactions and hydrogen bonding. Bonhôte et al.[39] stated in their work that charge delocalization within the anion weakens intermolecular hydrogen bonding with the cation, leading to lower viscosities if not overcompensated by van der Waals interactions. For the ILs containing the [EMIM]-cation, the highest viscosity found for [EMIM][$OcSO_4$] can be explained with the long side chain of the anion, which increases the contributions to viscosity by entanglement and van der Waals interactions. It is worth mentioning that the ILs [EMIM][$MeSO_3$] and [EMIM][$MeOHPO_2$] exhibit higher viscosities compared to the previously investigated [EMIM][$EtSO_4$].[13] For the latter, a higher viscosity would be expected, because the ethyl side chain length is larger compared to the methyl side chain length enhancing van der Waals forces. Yet, also the basicity, the strength of the negative charge of the anion, has an effect on the thermophysical properties.[39] In [EMIM]-based ILs, more

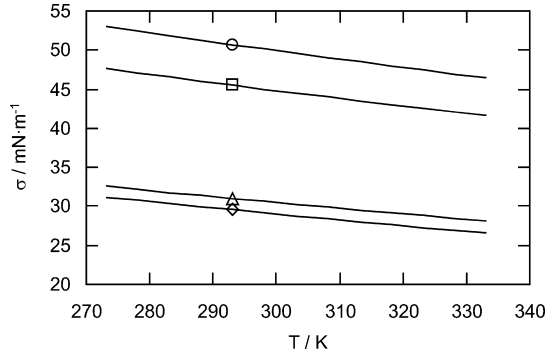

Figure 3. Interfacial tension σ of ionic liquids at atmospheric pressure as a function of temperature: ○, [EMIM][$MeSO_3$]; □, [EMIM][$MeOHPO_2$]; △, [EMIM][$OcSO_4$]; ◇, [BBIM][NTf_2].

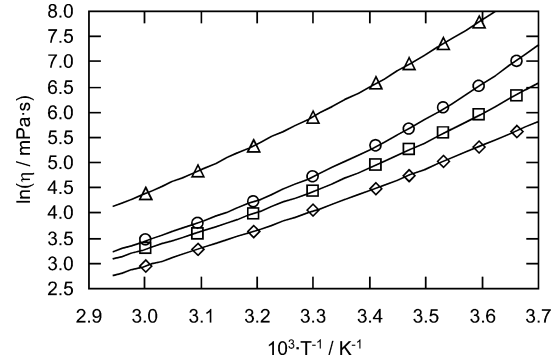

Figure 4. Arrhenius plots of dynamic viscosity η for ionic liquids: ○, [EMIM][$MeSO_3$]; □, [EMIM][$MeOHPO_2$]; △, [EMIM][$OcSO_4$]; ◇, [BBIM][NTf_2].

Table 7. Dynamic Viscosity η of Ionic Liquids [EMIM][$MeSO_3$], [EMIM][$MeOHPO_2$], [EMIM][$OcSO_4$], and [BBIM][NTf_2] from T = (273.15 to 333.15) K at Atmospheric Pressure[a]

	[EMIM][$MeSO_3$]	[EMIM][$MeOHPO_2$]	[EMIM][$OcSO_4$]	[BBIM][NTf_2]
T/K	η/mPa·s	η/mPa·s	η/mPa·s	η/mPa·s
273.15	1112.6	563.9	3894.8	277.9
278.15	676.3	379.6	2429.9	203.0
283.15	435.5	266.6	1578.5	152.1
288.15	290.1	193.2	1045.1	115.3
293.15	205.2	143.1	717.8	89.5
303.15	112.9	83.4	368.1	57.2
313.15	69.0	53.9	208.1	37.9
323.15	44.6	36.4	126.2	26.5
333.15	31.7	27.4	80.9	19.2

[a] Directly measured values of the mean decay time τ_C at a defined wave vector q of surface fluctuations were combined with interfacial tension data σ, eq 6, and density data ρ, eq 5. using coefficients from Table 5, to derive η by an exact numerical solution of the dispersion relation eq 1.

Table 8. Coefficients of Equation 7 for the Viscosity of Ionic Liquids [EMIM][$MeSO_3$], [EMIM][$MeOHPO_2$], [EMIM][$OcSO_4$], and [BBIM][NTf_2] Listed in Table *7*

	[EMIM][$MeSO_3$]	[EMIM][$MeOHPO_2$]	[EMIM][$OcSO_4$]	[BBIM][NTf_2]
η_0/mPa·s	0.37623	0.27273	0.06946	0.05918
B/K	596.447	688.941	1194.118	1098.279
C/K	198.534	182.993	163.997	143.230
rms[a]	0.57	1.24	0.44	0.31

[a] Standard percentage deviation of η to the fit.

basic anions lead to tighter ion pairing of the cation with the anion, which also increases intermolecular forces like hydrogen bonding. The [$EtSO_4$]-anion exhibits the lowest basicity, followed by the [$MeOHPO_2$]- and the [$MeSO_3$]-anion, which is in agreement with the order of the viscosity of the three ILs. The IL [EMIM][NTf_2] shows the lowest viscosity of the [EMIM]-based ILs investigated in this and the previous work.[13] This can be explained with the disability of the [NTf_2]-anion to interact in the form of hydrogen bonding and a randomized aggregation of ions caused by very low anionic basicity.[39] Also for the comparison of different ILs containing the [NTf_2]-anion, [EMIM][NTf_2] exhibits the lowest viscosity, followed by [BBIM][NTf_2] and [OMA][NTf_2]. It is evident that a higher viscosity is caused by an increasing alkyl chain length of the cation.

For the viscosity of [EMIM][$MeSO_3$], two data points are available in the literature. Himmler et al.[31] determined a viscosity of 207 mPa·s at 298.15 K and atmospheric pressure for a sample with a purity > 99 % and a water content of 980 ppm. They used a rotational viscometer (Anton Paar, MCR 100), where the sample was processed under an argon atmosphere, and the temperature was controlled via a Peltier element. The authors give no information about the uncertainty of their measurements. Cooper and O'Sullivan[30] measured a viscosity of 160 mPa·s at 298 K and atmospheric pressure using a capillary viscometer. They do not specify the purity of the sample, its water content, and the uncertainty of their measurements. The value of Himmler et al.[31] deviates about 38 % from the correlation, eq 7, of this work. This difference can not be explained by the water content of their sample, which was about 330 ppm lower than in this work. The value of Cooper and O'Sullivan[30] deviates 5.8 % from our data correlation. For [EMIM][$MeOHPO_2$], only one datum is available from Fukaya et al.,[40] who measured a viscosity of 107 mPa·s at 293.15 K. The authors specify the water content to be lower than 1000 ppm, yet they do not provide information about the measurement technique and its uncertainty. Their value, however, deviates about 1 % from the data correlation, eq 7, of this work. In Figure 5, the results for the dynamic viscosity of [EMIM][$OcSO_4$] from SLS are shown together with data from Himmler et al.[17] They have studied the viscosity of [EMIM][$OcSO_4$] for temperatures between (293.15 and 373.15) K in intervals of 10 K with a rotational viscometer (Anton Paar, MCR 100). Their sample had a nominal purity of 99 % and a water content of (600 ± 100) ppm. As for [EMIM][$MeSO_3$], Himmler et al.[17] give no information about the measurement uncertainty. For the comparison, the correlation of our data, eq 7, serves as a basis. As can be seen from Figure 5, the data of Himmler et al.[17] deviate between −10 % at 293.15 K and +2.5 % at 333.15 K. These deviations can not be attributed to the difference in the water content, which was for their sample about 500 ppm by mass lower than for our sample. Due to the lack of literature data, a data comparison for the viscosity of [BBIM][NTf_2] could not be drawn.

Conclusions

This work presents the investigation of several thermophysical properties of four imidazolium-based ILs, namely, [EMIM][$MeSO_3$], [EMIM][$MeOHPO_2$], [EMIM][$OcSO_4$], and [BBIM][NTf_2], in dependence on temperature at atmospheric pressure. The experimental data for the refractive index, density, interfacial tension, and viscosity were discussed qualitatively in connection with structural variations of the cations and anions in the ILs. In addition, a comparison with the literature was

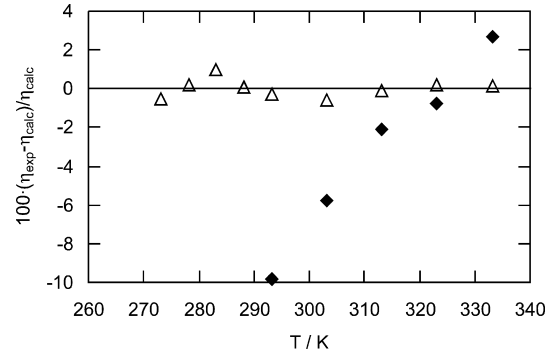

Figure 5. Comparison between the dynamic viscosity η of [EMIM][$OcSO_4$] at atmospheric pressure for temperatures between (273.15 and 333.15) K (−, eq 7 using coefficients from Table 8): △, this work; ◆, Himmler et al.[17]

drawn, yet at present only a scarce data situation can be found for the ILs investigated. The disagreements between different data sources may be attributed to an inconsistent sample purity and unspecified experimental conditions, yet this seems not to be the only reason. Here, the discrepancies for the physicochemical properties, including equilibrium properties, originating from different sources were also found to be influenced by inconsistent experimental techniques as well as an inadequate estimation of their uncertainty.

Literature Cited

(1) Balducci, A.; Soavi, F.; Mastragostino, M. The use of ionic liquids as solvent-free green electrolytes for hybrid supercapacitors. *Appl. Phys. A: Mater. Sci. Process.* **2006**, *82*, 627–632.

(2) Van Valkenburg, M. E.; Vaughn, R. L.; Williams, M.; Wilkes, J. S. Thermochemistry of ionic liquid heat-transfer fluids. *Thermochim. Acta* **2005**, *425*, 181–188.

(3) Welton, T. Room-temperature ionic liquids. Solvents for synthesis and catalysis. *Chem. Rev.* **1999**, *99*, 2071–2083.

(4) Wasserscheid, P.; Keim, W. Ionic liquids - New 'solutions' for transition metal catalysis. *Angew. Chem., Int. Ed.* **2000**, *39*, 3773–3789.

(5) Schroer, K.; Tacha, E.; Lutz, S. Process intensification for substrate-coupled whole cell ketone reduction by in situ acetone removal. *Org. Process Res. Dev.* **2007**, *11*, 836–841.

(6) Fukushima, T.; Aida, T. Ionic liquids for soft functional materials with carbon nanotubes. *Chem.—Eur. J.* **2007**, *13*, 5048–5058.

(7) Wei, D.; Ivaska, A. Applications of ionic liquids in electrochemical sensors. *Anal. Chim. Acta* **2008**, *607*, 126–135.

(8) Widegren, J. A.; Laesecke, A.; Magee, J. W. The effect of dissolved water on the viscosities of hydrophobic room temperature ionic liquids. *Chem. Commun.* **2005**, 1610–1612.

(9) Seddon, K. R.; Stark, A.; Torres, M. J. Influence of chloride, water, and organic solvents on the physical properties of ionic liquids. *Pure Appl. Chem.* **2000**, *72*, 2275–2287.

(10) Perry, R. L.; Jones, K. M.; Scott, W. D.; Liao, Q.; Hussey, C. L. Densities, viscosities, and conductivities of mixtures of selected organic cosolvents with the lewis basic aluminum chloride + 1-methyl-3-ethylimidazolium chloride molten salt. *J. Chem. Eng. Data* **1995**, *40*, 615–619.

(11) Huddleston, J. G.; Visser, A. E.; Reichert, W. M.; Willauer, G. A.; Rogers, R. D. Characterization and comparison of hydrophilic and hydrophobic room temperature ionic liquids incorporating the imidazolium cation. *Green Chem.* **2001**, *3*, 156–164.

(12) Poole, C. F.; Kersten, B. R.; Ho, S. S. J.; Coddens, M. E.; Furton, K. G. Organic salts, liquid at room temperature, as mobile phases in liquid chromatography. *J. Chromatogr.* **1986**, *352*, 407–425.

(13) Fröba, A. P.; Kremer, H.; Leipertz, A. Density, refractive index, interfacial tension, and viscosity of ionic liquids [EMIM][$EtSO_4$], [EMIM][NTf_2], [EMIM][$N(CN)_2$], and [OMA][NTf_2] in dependence on temperature at atmospheric pressure. *J. Phys. Chem. B* **2008**, *112*, 12420–12430.

(14) Fröba, A. P.; Leipertz, A. Accurate determination of liquid viscosity and surface tension using surface light scattering (SLS): Toluene under saturation conditions between 260 and 380 K. *Int. J. Thermophys.* **2003**, *24*, 895–921.

(15) Fröba, A. P.; Leipertz, A. Viscosity of diisodecyl phthalate by surface light scattering (SLS). *J. Chem. Eng. Data* **2007**, *52*, 1803–1810.

(16) Fröba, A. P.; Leipertz, A. Accurate determination of dynamic viscosity of high-viscosity fluids using surface light scattering (SLS). *Int. J. Thermophys.*, to be submitted for publication.

(17) Himmler, S.; Hörmann, S.; van Hal, R.; Schulz, P. S.; Wasserscheid, P. Transesterification of methylsulfate and ethylsulfate ionic liquids - an environmentally benign way to synthesize long chain and functionalized alkylsulfate ionic liquids. *Green Chem.* **2006**, *8*, 887–894.

(18) Davis, J. H., Jr.; Gordon, C. M.; Hilgers, C.; Wasserscheid, P. Synthesis and purification of ionic liquids. In *Ionic Liquids in Synthesis*; Wasserscheid, P., Welton, T., Eds.; Wiley-VCH: Weinheim, Germany, 2006; pp 7−13.

(19) Levich, V. G. *Physicochemical Hydrodynamics*; Prentice Hall: Englewood Cliffs, 1962.

(20) Fröba, A. P.; Botero, C.; Leipertz, A. Investigation of high-viscosity fluids by surface light scattering (SLS) passing the critical damping of surface fluctuations. *J. Appl. Phys.*, to be submitted for publication.

(21) Lucassen-Reynders, E. H.; Lucassen, J. Properties of capillary waves. *Adv. Colloid Interface Sci.* **1969**, *2*, 347–395.

(22) Langevin, D. *Light Scattering by Liquid Surfaces and Complementary Techniques*; Marcel Dekker: New York, 1992.

(23) Fröba, A. P. Simultane Bestimmung von Viskosität und Oberflächenspannung transparenter Fluide mittels Oberflächenlichtstreuung, Dr.-Ing. thesis, Friedrich-Alexander-Universität Erlangen-Nürnberg, Germany, 2002.

(24) Deetlefs, M.; Seddon, K. R.; Shara, M. Predicting physical properties of ionic liquids. *Phys. Chem. Chem. Phys.* **2006**, *8*, 642–649.

(25) Brocos, P.; Piñeiro, Á.; Bravo, R.; Amigo, A. Refractive indices, molar volumes and molar refractions of binary liquid mixtures: Concepts and correlations. *Phys. Chem. Chem. Phys.* **2003**, *5*, 550–557.

(26) Arce, A.; Rodríguez, H.; Soto, A. Effect of anion fluorination in 1-ethyl-3-methylimidazolium as solvent for the liquid extraction of ethanol from ethyl tert-butyl ether. *Fluid Phase Equilib.* **2006**, *242*, 164–168.

(27) Deenadayalu, N.; Ngcongo, K. C.; Letcher, T. M.; Ramjugernath, D. Liquid-liquid equilibria for ternary mixtures (an ionic liquid + benzene + heptane or hexadecane) at $T = 298.2$ K and atmospheric pressure. *J. Chem. Eng. Data* **2006**, *51*, 988–991.

(28) Fredlake, C. P.; Crosthwaite, J. M.; Hert, D. G.; Aki, S. N. V. K.; Brennecke, J. F. Thermophysical properties of imidazolium-based ionic liquids. *J. Chem. Eng. Data* **2004**, *49*, 954–964.

(29) Tokuda, H.; Hayamizu, K.; Ishii, K.; Susan, M. A. B. H.; Watanabe, M. Physicochemical properties and structures of room temperature ionic liquids. 2. variation of alkyl chain length in imidazolium cation. *J. Phys. Chem. B* **2005**, *109*, 6103–6110.

(30) Cooper, E. I.; O'Sullivan, E. J. M. New, stable, ambient-temperature molten salts. In *Proceedings of the 8th International Symposium on Molten Salts*; Gale, R. J., Blomgren, G., Eds.; The Electrochemical Society: Pennington, NJ, 1992; Vol. 92-16, pp 386−396.

(31) Himmler, S.; König, A.; Wasserscheid, P. Synthesis of [EMIM]OH *via* bipolar membrane electrodialysis - precursor production for the combinatorial synthesis of [EMIM]-based ionic liquids. *Green Chem.* **2007**, *9*, 935–942.

(32) Reid, R. C.; Prausnitz, J. M.; Poling, B. E. *The Properties of Gases and Liquids*; McGraw-Hill: New York, 1987.

(33) MacLeod, D. B. On a relation between surface tension and density. *Trans. Faraday Soc.* **1923**, *19*, 38–41.

(34) Sugden, S. The variation of surface tension with temperature and some related functions. *J. Chem. Soc., Trans.* **1924**, *125*, 32–41.

(35) Law, G.; Watson, P. R. Surface tension measurements of n-alkylimidazolium ionic liquids. *Langmuir* **2001**, *17*, 6138–6141.

(36) Tokuda, H.; Tsuzuki, S.; Susan, M. A. B. H.; Hayamizu, K.; Watanabe, M. How ionic are room-temperature ionic liquids? An indicator of the physicochemical properties. *J. Phys. Chem. B* **2006**, *110*, 19593–19600.

(37) Knotts, T. A.; Wilding, W. V.; Oscarson, J. L.; Rowley, R. L. Use of the DIPPR database for development of QSPR correlations: Surface tension. *J. Chem. Eng. Data* **2001**, *46*, 1007–1012.

(38) Sewell, J. H. A method of calculating densities of polymers. *J. Appl. Polym. Sci.* **1973**, *17*, 1741–1747.

(39) Bonhôte, P.; Dias, A. P.; Papageorgiou, N.; Kalyanasundaram, K.; Grätzel, M. Hydrophobic, highly conductive ambient-temperature molten salts. *Inorg. Chem.* **1996**, *35*, 1168–1178.

(40) Fukaya, Y.; Hayashi, K.; Wada, M.; Ohno, H. Cellulose dissolution with polar ionic liquids under mild conditions: required factors for anions. *Green Chem.* **2008**, *10*, 44–46.

Received for review January 30, 2009. Accepted March 7, 2009. This work was supported by the German National Science Foundation (Deutsche Forschungsgemeinschaft, DFG) via the DFG-SPP1191 priority program and by the Max-Buchner-Forschungsstiftung.

JE900134Z